Membrane Properties of Antiviral Phospholipids Containing Heteroatoms in the Acyl Chains†

Xiaoxing Qiu and Charles Pidgeon*

Department of Medicinal Chemistry and Pharmacognosy, School of Pharmacy, Purdue University, West Lafayette, Indiana 47907

Received June 21, 1993; Revised Manuscript Received November 8, 1993®

ABSTRACT: Phospholipids containing heteroatoms in the lipid acyl chains, e.g., 1,2-bis(12-methoxydodecanoyl)-*sn*-3-phosphocholine (L-AC2), exhibit potent anti-HIV activity [Pidgeon, C., Markovich, R. J., Liu, M. D., Holzer, T., Novak, R., & Keyer, K. (1993) *J. Biol. Chem.* 268, 7773–7778]. AC2 is a synthetic chemical analog of the long-chain phospholipid, dimyristoylphosphatidylcholine (DMPC). Sonicated AC2 lipid dispersions would not entrap either Dextran-4000 or Mn^{2+} used as aqueous space markers. The lack of entrapment of aqueous space markers indicates that the AC2 structures do not contain an aqueous core that is the characteristic morphology of conventional lipid vesicles formed by sonication. Transmission electron microscopy (TEM) showed that sonicated AC2 lipid dispersions are small homogeneous particles approximately 70–100 Å in diameter. ^1H NMR experiments using Mn^{2+} as a broadening reagent indicated that Mn^{2+} was accessible to all of the AC2 phospholipid headgroups in the AC2 lipid particles formed by sonication. The temperature dependence of ^1H spin-lattice (T_1) relaxation time measurements revealed that the motional activation energies increased from the choline headgroup to the end of the acyl chains of AC2 molecules in the AC2 lipid particles formed by sonication. Collectively these results demonstrate that AC2 forms micelles. NOESY experiments showed that the AC2 molecules forming the micelle structures have hindered motion compared to conventional short-chain phosphatidylcholine micelles. ^{31}P NMR spectroscopy and TEM showed that the AC2 micelles extensively fuse into giant bilayer liposomes (single-layered) when the temperature is reduced from above to below the main phase transition temperature of AC2. This micelle-to-liposome transition is an irreversible process; increasing the temperature above the T_m does not cause the formation of micelles. Thus, a main finding is that AC2 micelles formed by sonication are not thermodynamically stable because they fuse into large unilamellar vesicles that are stable to further changes in temperature. These unusual membrane properties of sonicated AC2 dispersions may be important for the antiviral activity and metabolism of the phospholipids.

Recently, a new class of synthetic phospholipids with activity against HIV-infected cells has been reported (Pidgeon et al., 1993). This potentially new therapeutic class of compounds is denoted as HAC phospholipids because the phospholipids contain heteroatoms in the acyl chains. Among the HAC phospholipids, 1,2-bis(12-methoxydodecanoyl)-*sn*-3-glycerophosphocholine (AC2[1]) is one of the most anti-HIV active compounds, with an IC_{50} of 1.0 μM. More significant is that AC2 exhibits potent synergism with AZT; the antiviral selectivity in combination therapy of AC2 and AZT is $\sim 10^4$, which is similar to many currently used drugs (Pidgeon et al., 1993).

All HAC phospholipids synthesized to date have been prepared from 12-methoxydodecanoic acid (12MO), which is a fatty acid reported to function as an alternative substrate for myristic acid during protein myristoylation (Bryant et al., 1989, 1991; Heuckeroth & Gordon, 1989). If 12MO is cleaved from HAC phospholipids by endogenous phospholipases (e.g., PLA_1 or PLA_2), then the antiviral mechanism of action would involve the inhibition of myristoylation of HIV proteins. However, since the L- and D-phospholipid isomers have similar activity (Pidgeon et al., 1993), the antiviral activity does not depend on PLA_2 enzymatically liberating 12MO *in situ*. PLA_1 has been reported to lack stereospecificity for antiviral phospholipids containing AZT tethered to the polar headgroup (Kumar et al., 1992), and therefore PLA_1 cleavage of L and D isomers of HAC phospholipids could also give rise to 12MO *in situ*. However, the anti-HIV phospholipids synthesized by Hermann (1993) suggest that mechanisms other than "alternative substrates of myristic acid" are participating in the antiviral activity of HAC phospholipids. Hermann's phospholipids were synthesized by linking saturated hydrocarbon chains to the glycerol backbone of glycerophosphocholine via ether bonds (*O*-alkylphospholipids) or thiol bonds (*S*-alkylphospholipids). Thus, these phospholipids are not substrates for either PLA_1 or PLA_2. In addition, these *O*-alkyl- and *S*-alkylphospholipids do not contain heteroatoms distal in the alkyl chains as do HAC phospholipids. The anti-HIV activity of Hermann's ether phospholipids measured in human T-lymphoma cells or fetal lung cells varies from an IC_{50} of ~1 to 10 μM, which is very similar to the values for HAC

† This research was supported in part by grants from the NSF (CTS 9214794) and NIH (AI33031).

* Address correspondence to this author.

® Abstract published in *Advance ACS Abstracts,* January 1, 1994.

[1] Abbreviations: AZT, azidothymidine; DMPC, dimyristoylphosphatidylcholine; AC2, same as L-AC2; L-AC2, 1,2-bis(12-methoxydodecanoyl)-*sn*-3-glycerophosphocholine; D-AC2, 2,3-bis(12-methoxydodecanoyl)-*sn*-1-glycerophosphocholine; DMAP, (dimethylamino)pyridine; 12MO, 12-methoxydodecanoic acid; EDTA, ethylenediaminetetraacetic acid; DCC, dicyclohexylcarbodiimide; TSP-d_4, sodium 3-(trimethylsilyl)-propionate-d_4; T_m, main transition temperature; SUV, small unilamellar vesicle; TEM, transmission electron microscopy; MeOH, methanol; MLV, multilayered vesicle; NOE, nuclear Overhauser effect; NOESY, two-dimensional NOE spectroscopy; vesicle, small single-layered liposome; L-PE2, 1,2-bis(12-methoxydodecanoyl)-*sn*-3-glycerophosphoethanolamine; L-PE1, 1-myristoyl-2-(12-methoxydodecanoyl)-*sn*-3-glycerophosphoethanolamine; HAC, heteratoms in the acyl chains; PLA_2, phospholipase A_2; PLA_1, phospholipase A_1; IC_{50}, drug concentration needed to reduce the infectivity of HIV by 50%; E_a, energy of activation.

0006-2960/94/0433-960$04.50/0

phospholipids. On the basis of the activity of Hermann's compounds, it is likely that additional antiviral mechanisms are participating in the activity of HAC phospholipids besides the putative inhibition of myristoylation of HIV proteins.

Aside from the antiviral mechanism of action, the stability in biological tissues of HAC phospholipids is expected to depend significantly on enzymatic processing by endogenous phospholipases. Enzymatic processing can alter the lipid headgroup, deacylate and reacylate the acyl chains, or completely catabolize the HAC phospholipids. Thus, both the metabolism of HAC phospholipids and the release of the biologically active heteroatom fatty acid from the HAC phospholipids will be determined by phospholipases. Phospholipase activity significantly depends on the structure of the lipid aggregate and the dynamics of the phospholipid in the aggregate (Bian & Roberts, 1990; Gabriel & Roberts, 1987; DeBose & Roberts 1983; El-Sayed et al., 1985). Thus, to understand both the antiviral mechanism of action and the metabolism of HAC phospholipids, it is necessary to elucidate their membrane-surface properties.

In this study, we compared the membrane properties of sonicated AC2 and DMPC lipid dispersions above the T_m of AC2. Sonication of aqueous AC2 dispersions results in the formation of micelles, but the micelles fuse into large liposomes when the temperature is reduced below this main transition temperature of AC2. Micelle formation by AC2 was unexpected because AC2 is a long-chain phospholipid similar to DMPC. This unusual property of micelle formation may play a role in the antiviral activity by altering the host plasma membrane and/or viral membrane. Our suggestion that HAC phospholipids exhibit antiviral activity from membrane perturbation is consistent with a recent report demonstrating that small hydrophobic peptides inhibit several enveloped viruses (e.g., measles and herpes simplex) by a mode of action based on the inhibition of membrane fusion between the host cell and the virus (Yeagle et al., 1992).

MATERIALS AND METHODS

Materials. DMPC was purchased from Avanti Polar Lipids and used as received. DMAP obtained from Aldrich was recrystallized from ethyl acetate as described (Pidgeon & Venkatarum, 1989). Sodium methoxide and 12-bromododecanoic acid (97%), used to prepare 12-methoxydodecanoic acid, were purchased from Aldrich and used as received. DCC, EDTA, and $MnCl_2$ were also obtained from Aldrich. 12MO anhydride was prepared by condensing 12MO (7.6 g, 0.0307 mol) with DCC (3.51 g, 0.017 04 mol) in 10 mL of dry THF for 1 h. The reaction mixture was filtered through a medium glass filter to removed dicylohexylurea, and then it was filtered through a fine glass filter. The solvent was evaporated, and the anhydride, obtained in >99% yield, was used without further purification for the synthesis of AC2. Anhydrous chloroform was obtained from Aldrich as a sure seal bottle and used without further drying. D_2O and 3-(trimethylsilyl)-propionic-*2,2,3,3-d*$_4$ acid, sodium salt (TSP-*d*$_4$), were obtained from Aldrich. Fluorescein isothiocyanate dextrans (MW 4000, Dextran-4000) and Sephadex G-200 were purchased from Sigma. IAM.PC$^{C10/C3}$ was purchased from Regis Chemical Company.

Synthesis of 1,2-Bis(12-methoxydodecanoyl)-sn-3-glycerophosphocholine (L-*AC2*) *and 2,3-Bis(12-methoxydodecanoyl)-sn-1-glycerophosphocholine* (D-*AC2*). Both the natural configuration (L-AC2) and the unnatural configuration (D-AC2) were synthesized by the same method using a novel solid-phase adsorption synthetic procedure developed in our lab (Pidgeon et al., 1993). Briefly, L-glycero-3-phosphocholine (natural configuration) or D-glycero-3-phosphocholine (unnatural configuration) dissolved in methanol was adsorbed to the surface of IAM.PC$^{C10/C3}$, and the residual methanol was removed by vacuum. The acylation was initiated by the addition of 12-methoxydodecanoyl anhydride (2 equiv per alcohol) dissolved in anhydrous $CHCl_3$; 2 equiv of (dimethylamino)pyridine was used to accelerate the reaction. The reactions were usually complete within 2–4 h; reaction yields were >80%. AC2 was pure based on thin-layer chromatography on silica gel plates using $CHCl_3$/MeOH/H_2O (65:25:4) as the mobile phase. Chemical structures were confirmed by ^{1}H NMR and mass spectrometry. When not explicitly stated (e.g., AC2), the stereochemistry of HAC phospholipids contains the natural L configuration at the glycero backbone. The unnatural D configuration is always stated; hence, D-AC2 is a phosphatidylcholine analog containing 2 equiv of the heteroatom fatty acid 12MO.

Lipid Dispersions. Phospholipid films were predried on the floor of a round-bottom flask from chloroform solutions of the phospholipids by rotary evaporation at 45 °C. Multilayered liposomes (MLVs) were prepared by adding aqueous media and vortexing above the T_m of each lipid at a lipid concentration of ~5–15 mg/mL.

Sonicated lipid dispersions were prepared by bath sonication. Multilayered liposomes were sonicated in a Branson 2200 (Fisher Scientific) bath sonicator above the main transition temperature of the lipid under a nitrogen atmosphere. The sonication was for at least 30 min but usually 1 h. Thin-layer chromatography using silica gel plates developed with the mobile phase $CHCl_3$/MeOH/H_2O (65:25:4) was used to evaluate lipid degradation; no degradation during sonication was ever found using Phospray (Supelco) to visualize the lipids. This solvent system was used to routinely check the stability of the lipids after each experiment. The lipid concentration in the final lipid dispersion for TEMs and ^{31}P NMR studies was 15 mg/mL; ^{1}H NMR studies utilized ~5 mg/mL.

Measurement of Internal Trapped Aqueous Volume. Two methods were used to evaluate whether the AC2 lipid particles formed by sonication contained an aqueous compartment: (i) entrapment of Dextran-4000 (a large aqueous space marker) and (ii) entrapment of Mn^{2+} (a small aqueous space marker, described below). For measuring the entrapment of Dextran-4000, MLVs were prepared using approximately 10 mg of either DMPC or AC2 in 1 mL of 1.36 mM Dextran-4000 buffer containing 5 mM Tris-HCl and 100 mM NaCl (pH 7.0). The MLV suspension was then sonicated for 30–60 min. After sonication, the lipid dispersions were fractionated on a Sephadex G200 column preequilibrated to either 50 °C for AC2 dispersions or 30 °C for DMPC dispersions. The elution buffer contained 5 mM Tris-HCl and 100 mM NaCl. One-milliliter fractions were collected from the Sephadex column and analyzed for fluorescently labeled Dextran-4000 using a thermostated cuvette holder, as described below. Fluorescence was measured on a Hitachi F-2000 fluorescence spectrophotometer with an excitation wavelength of 490 nm and an emission wavelength of 516 nm. Fluorescent measurements were obtained at 45 °C for AC2 or 35 °C for DMPC.

In contrast to using both Dextran-4000 and Mn^{2+} to measure the aqueous compartments of AC2 particles formed by sonication, only Dextran-4000 was used to monitor the aqueous compartment of the large liposomes formed by the fusion of AC2 micelles. Small AC2 particles were prepared at 50 °C, as described above using buffer containing Dextran-4000. Fusion was initiated by reducing the temperature to 35 °C,

and the sample was maintained at 35 °C for 30 min. Fusion causes the formation of large liposomes that entrap Dextran-4000 during the fusion event; un-entrapped Dextran-4000 was separated from the large liposomes by pelleting in a microfuge (10 min at 14000*g*) and then washing the liposome pellet by resuspension in buffer. Liposomal pellets were washed five times. The final pellet was resuspended in buffer to a final volume of 1 mL. Before the amount of liposome-encapsulated Dextran-4000 was quantitated by fluorescence, the background light scattering from the AC2 liposomes themselves was eliminated by merely sonicating the suspension for 30 min to obtain a clear solution. The sonicated dispersion was diluted 10 times before fluorescence measurements were recorded at 45 °C. Phospholipid recoveries after pelleting are ~98%. The liposomal entrapped volumes are the microliters of aqueous trapped volume (based on Dextran-4000) per micromole of total lipid.

Measurement of Internal Aqueous Volume Using Mn^{2+}. Small lipid particles formed by sonication exhibit high-resolution ^{1}H NMR spectra because the small lipid particles tumble rapidly, and there also exist rapid internal motions of the phospholipid molecules on the NMR time scale. Mn^{2+} is a paramagnetic broadening reagent, and for chemical groups that have access to Mn^{2+}, the proton spectral intensities are significantly broadened or eliminated. Our Mn^{2+} broadening experiments are similar to earlier studies (Schuh et al., 1982) that used this method to probe the external and internal phospholipid populations. DMPC and AC2 sonicated dispersions were prepared without Mn^{2+} (condition A), with Mn^{2+} 'outside' the vesicles only (condition B), with Mn^{2+} 'inside' and 'outside' the vesicles (condition C), and with Mn^{2+} 'inside' and 'outside' the vesicles but with EDTA added to the bulk aqueous volume. For conditions A–D, the single quotes encompassing 'inside' and 'outside' emphasize where the Mn^{2+} resides if an internal aqueous compartment exists in the lipid particles. For consistency, these single quotes are used for all lipid dispersions even though some of the lipid dispersions formed micelles. Each phospholipid was initially dispersed by mild vortexing in 2 mL of 90 mM NaCl and then sonicated as described above to prepare enough of the lipid dispersion to take aliquots for dilution with paramagnetic broadening agents.

For condition A, 400 μL of the initial 2-mL total dispersion volume was diluted with an equal volume of 90 mM NaCl for ^{1}H NMR spectral measurements. For condition B, a 400-μL aliquot of the 2-mL dispersion volume was diluted with a 90 mM NaCl solution containing 0.5 mM $MnCl_2$. For condition C, a 400-μL aliquot of the 2-mL lipid dispersion volume was diluted as in condition A, except that 0.5 mM $MnCl_2$ was included in both the initial aqueous dispersion solution and the dilution solution used to dilute the lipid dispersion. For condition D, a 400-μL aliquot of the 2-mL lipid dispersion was treated exactly as for condition C, but it was then diluted with an equal volume of 60 mM EDTA. ^{1}H NMR spectra were obtained as described below.

NMR Measurements. All spectra were recorded on a Varian VXR 500 spectrometer operating at a field strength of 11.7 T. The temperature was controlled to an accuracy of ±0.5 °C, and the time allowed for temperature equilibration was ~15–30 min. Chemical shifts were referenced to TSP-d_4 (0.00 ppm) for ^{1}H NMR resonance and to 85% H_3PO_4 (0.0 ppm) for ^{31}P NMR resonance. All Mn^{2+} broadening experiments using ^{1}H as the observation nucleus were carried out at 50 °C. Spectra were obtained using a single 90° pulse (10 μs) and a 6-s repetition delay time. Solvent suppression was achieved by irradiation of the HDO resonance during the relaxation delay. ^{1}H NMR spectra of sonicated dispersions were obtained from 16 transients, and a 1-Hz exponential window function was used before Fourier transformation.

^{1}H spin-lattice relaxation (T_1) times of sonicated AC2 and DMPC dispersions were measured as a function of temperature; the first temperature was above the T_m of the lipid and sequential measurements were performed at higher temperatures. T_1 times were determined using an inversion recovery ($\pi-\tau-\pi/2$) pulse sequence (Vold et al., 1968) without water suppression. The repetition delay times were 5 times longer than the relevant T_1 values. Typically, eight transients were collected, and a 0.5-Hz exponential window function was used before Fourier transformation.

^{31}P NMR experiments were carried out above and below the T_m's of each lipid sample using a completely phase-cycled Hahn echo pulse sequence (Rance & Byrd, 1983). Spectra were thus obtained using a pulse sequence of $\pi/2-\tau-\pi-\tau-$ echo, where the $\pi/2$ pulse width was 17 μs and the delay time τ was 40 μs. Gated WALTZ proton decoupling and a 4-s recycle time were used for all ^{31}P spectral measurements. Data were acquired over a 100 kHz spectral width and the total acquisition time was 0.2 or 0.05 s. Either 300 or 1500 transients were collected, depending on the sample concentration and peak intensity. The ^{31}P free induction decay was Fourier transformed with either a 100- or 200-Hz exponential weighting function (as stated in the figure legends).

Two-dimensional ^{1}H nuclear Overhauser effect spectroscopy (NOESY) experiments were carried out in the phase-sensitive mode (States et al., 1982) above the T_m of each lipid sample. The NOESY pulse sequence ($\pi/2-t_1-\pi/2-\tau_m-\pi/2-t_2$) was used with mixing times (τ_m) of 50–800 ms. The transmitter was set on the HDO resonance, and a 2-s presaturation was used to suppress the HDO resonance. Typically, 256 t_1 increments and a 300-ms mixing time were used for each experiment with eight transients per increment. In t_2, 2K data points were acquired over a spectral width of 3–3.6 kHz with a 4-s recycle time. All spectra were processed on a SUN Sparc station. The data sets were multiplied by a shifted sine-bell weighting function in both dimensions and zero-filled to 2K data points in the t_1 dimension before Fourier transformation.

Measurement of T_m. The T_m's of the phospholipids were measured by differential scanning calorimetry using multilayered liposomes on a Perkin-Elmer differential scanning calorimeter equipped with a thermal analysis data station. Three separate specimens were used to obtain both the T_m and enthalpy (ΔH) of AC2, DMPC, and DPPC aqueous dispersions. A heating scan rate of 10 °C/min was used.

Transmission Electron Microscopy (TEM). Electron microscopy of negative-stained specimens was examined on carbon-coated formvar films on copper grids using a Phillips EM-400 electron microscope operating at 80 kV. Negative-stain samples were prepared by maintaining both the AC2 dispersions and 2% uranyl acetate staining solution at 50 °C using a water bath. Uranyl acetate staining was performed in a temperature-controlled room with the temperature set at 42 °C. This temperature control was needed to prevent fusion of AC2 lipid particles during sample preparation. For transmission electron micrographs (TEMs) of DMPC and AC2 obtained below 50 °C (see Figures 8 and 9), a water bath was used to control the temperature of both the liposomes and staining solutions.

Cryo-TEM was used to evaluate the liposomes that formed by the fusion of small AC2 lipid particles. Samples for cryo-TEM were prepared as described by Walter et al. (1991).

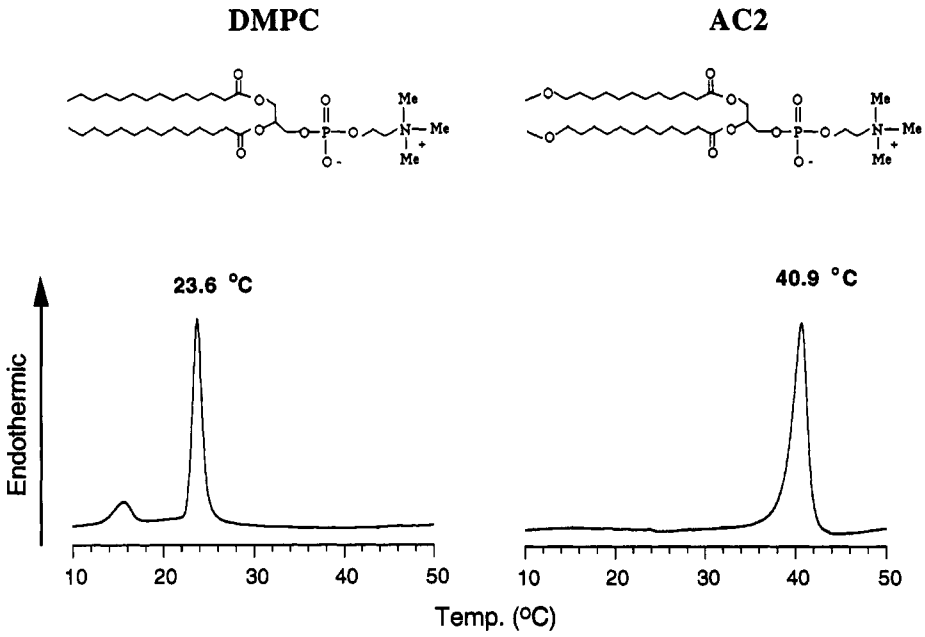

FIGURE 1: DSC heating thermograms of hydrated DMPC and AC2 (1 mg/20 μL). Heating rate: 10 °C/min.

Briefly, 4 μL of sonicated AC2 lipid dispersions incubated at 35 °C for 30 min was applied to a copper grid containing a small hole; the grid was carbon-coated. The lipid dispersion was immediately frozen using liquid ethane. The specimens were examined on a cryo-TEM cold stage using a Phillips EM-420 electron microscope operating at 80 kV.

RESULTS

The chemical structures of AC2 and DMPC differ only in the acyl chains tethered to glycerophosphocholine. DMPC has two saturated acyl chains, whereas AC2 has an oxygen atom at position C13 in both acyl chains (Figure 1). Differential scanning calorimetry of DMPC multilayered liposomes showed the expected pretransition peak at ~15 °C, whereas AC2 multilayer dispersions showed no evidence of a pretransition in the thermograms; only a main transition (T_m) was observed. Most striking is that the T_m of AC2 is 40.9 °C, which is ~18 °C higher than the T_m of DMPC (Figure 1). In addition, the ΔH of AC2 was 7.1 kcal/mol, which is ~2 kcal/mol higher than the ΔH of DMPC (ΔH = 5.0 kcal/mol). The increase in the T_m and ΔH of AC2 compared to those of DMPC clearly indicates that substitution an oxygen atom for a methylene group in the acyl chain can significantly influence the molecular packing of the lipids in the membrane. The molecular motion associated with the pretransition temperature involves a reorientation of the lipid molecules such that the acyl chains are tilted (relative to the membrane surface) below the pretransition temperature but reorient to a perpendicular position above the pretransition temperature. This phase change is called a ripple phase ($P_{\beta'}$) because the membrane surface appears rippled in electron micrographs. The lack of a pretransition for AC2 membranes suggests that the AC2 lipid molecules do not form membranes that can accommodate the $P_{\beta'}$ phase.

The structure of lipid particles formed by sonication was studied by ^{31}P NMR spectroscopy, TEM, and solute trapping experiments. We extensively utilized ^{31}P NMR spectroscopy because ^{31}P NMR spectral line shapes are sensitive to both the size and polymorphism (bilayer vs hexagonal phases) of lipid dispersions (Seelig, 1978; Cullis & de Kruijff, 1979). Early studies (Burnell et al., 1980) demonstrated that less than 1000 Å diameter vesicles exhibit a narrow symmetric resonance centered at 0 ppm with a 1.5 ppm line width at half-height ($\Delta\nu_{1/2}$) due to rapid tumbling of the lipid particle. As the vesicle's size increases, vesicle tumbling rates decrease, which causes the spectral line width to increase; furthermore, the line shape itself changes from an isotropic line shape to an axially symmetric powder pattern as the liposome size increases. For example, vesicles with a diameter of 5000 Å exhibit an axially symmetric line shape with a residual chemical shift anisotropy ($\Delta\sigma = \sigma_{\parallel} - \sigma_{\perp}$) of 25 ppm (Burnell et al., 1980). As shown in Figure 2, the ^{31}P NMR spectra of both sonicated AC2 and DMPC dispersions obtained above the T_m of each lipid show an isotropic resonance at 0 ppm with $\Delta\nu_{1/2}$ = 0.8 ppm. This isotropic line shape indicates that only small lipid particles (<1000 Å) exist in both sonicated AC2 and DMPC dispersions. TEM micrographs (Figure 2) show that sonicated DMPC lipid dispersions form well-defined spherical lipid particles that are homogeneous in size (~250 Å), whereas sonicated AC2 lipid dispersions generate much smaller lipid particles that are in the range of 70–100 Å in diameter.

Small AC2 lipid particles may be bilayer fragments, micelles, or vesicles. Bilayer fragments and micelles quantitatively have their phospholipid headgroups exposed or accessible to the bulk aqueous media. In contrast to micelles and bilayer fragments, vesicles have an inner and outer monolayer of lipid, and consequently, only the lipids in the outer monolayer have their polar headgroups accessible to the bulk aqueous medium. To probe the accessibility of AC2 lipid headgroups to the bulk aqueous medium, ^1H NMR spectroscopy was performed on the sonicated dispersions using Mn^{2+} as a broadening reagent (Schuh et al., 1982). As a control, DMPC SUVs (i.e., sonicated dispersions) were evaluated first, so that the expected changes in peak intensities in the presence and absence of Mn^{2+} could be unambiguously defined.

^1H NMR spectral resonances of DMPC SUVs depend on the lipid packing differences between the inner and outer monolayers of lipid (Schuh et al., 1982). Because of nonequivalent lipid packing, identical functional groups (e.g., the choline *N*-methyls) that reside in the inner monolayer are nonequivalent to the same chemical groups located in the

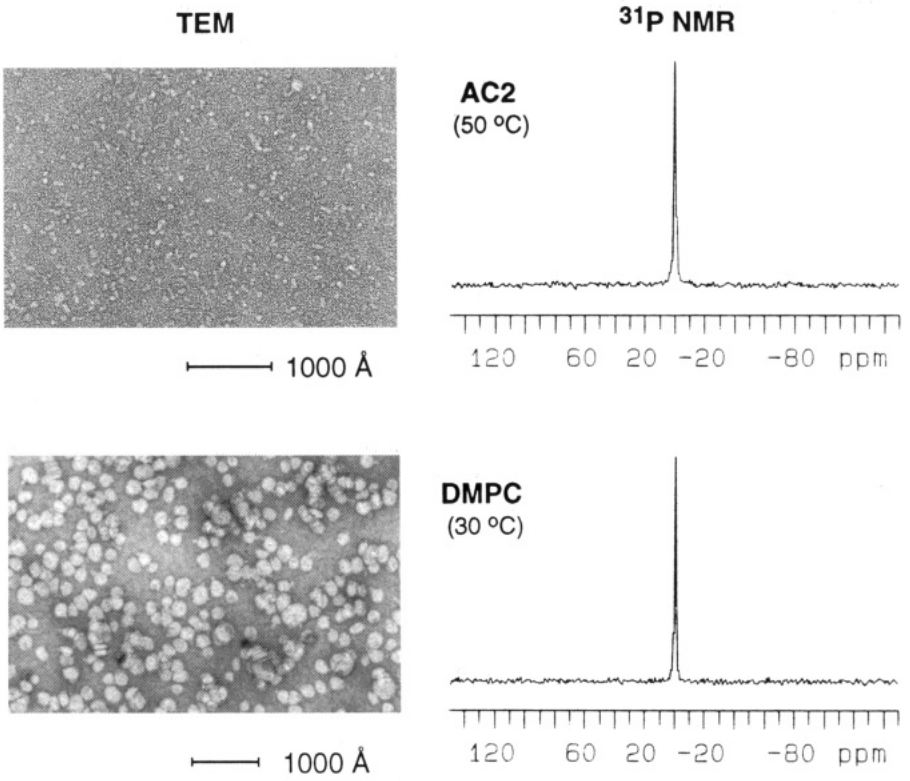

FIGURE 2: Negative-stain electron micrographs and 202-MHz ^{31}P NMR spectrum of sonicated AC2 and DMPC lipid dispersions above the T_m of each lipid. The AC2 spectrum was obtained at 50 °C with an acquisition time of 0.4 s and 300 transients. The DMPC spectrum was obtained at 30 °C with an acquisition time of 0.4 s and 200 transients. A 100-Hz line-broadening function was used for both spectra prior to Fourier transformation.

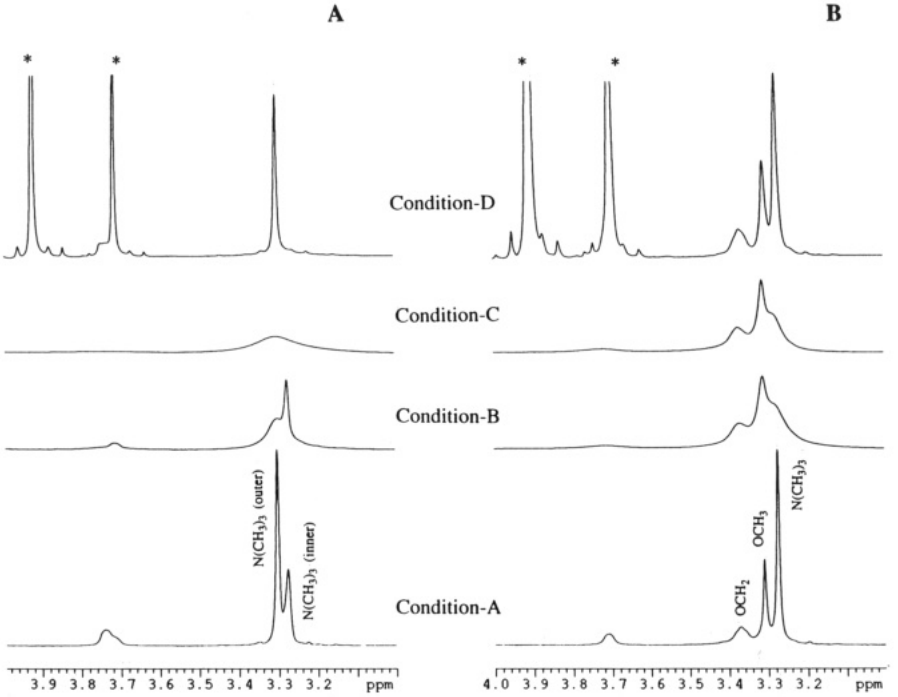

FIGURE 3: 500-MHz ^1H NMR spectra of sonicated DMPC (A) and AC2 (B) lipid dispersions in the presence and absence of Mn^{2+} at 50 °C. DMPC and AC2 dispersions were prepared without Mn^{2+} (condition A), with Mn^{2+} outside the liposomes only (condition B), with Mn^{2+} inside and outside the vesicles (condition C), and with Mn^{2+} inside and outside the vesicles with EDTA added to the extraliposomal bulk aqueous volume (condition D). For condition D, the sonicated lipid dispersion obtained from condition C was diluted with an equal volume of 60 mM EDTA. Chemical shift assignments are given in Table 1. The resonances from EDTA are labeled with an *.

outer monolayer; thus, most ^1H NMR resonances are doublets (Figure 3A (condition A) and Table 1). The high-field peak of each doublet corresponds to lipids on the inner monolayer (Schuh et al., 1982). The approximate ratio of molecules on the inner and outer monolayers of SUVs is ~1:2 (Pidgeon & Hunt, 1981), and peak intensities for each doublet should be approximately 1:2; integration of several of the ^1H NMR resonances gave approximately this ratio. Addition of Mn^{2+} to DMPC SUVs exposes only the outer monolayer of lipids to the paramagnetic ions. As expected, all of the DMPC headgroup resonances in the outer monolayer were broadened, and the resonances from the inner monolayer were unaffected

Table 1: ^{1}H Chemical Shift Assignments for Sonicated Lipid Dispersions[a]

chemical group	chemical shifts (ppm) DMPC	AC2
ω-CH_3	0.940	
$(CH_2)_n$	1.325 (i)[b]	1.362
	1.355 (o)[c]	
CH_2CH_2O		1.592
CH_2CH_2CO	1.655	1.620
CH_2CO	2.400	2.40
$N(CH_3)_3$	3.276 (i)	3.275
	3.303 (o)	
CH_3O		3.310
CH_2OCH_3		3.371
$POCH_2CH_2N$	3.702 (i)	3.700
	3.739 (o)	
$POCH_2CH_2N$	4.300 (i)	4.320
	4.352 (o)	
CHOCO	5.300 (i)	5.300
	5.340 (o)	

[a] All chemical shifts were referenced to TSP-d_4 at 0.00 ppm. [b] i indicates the resonance was from the inner monolayer of SUVs. [c] o indicates the resonance was from the outer monolayer of SUVs.

(Figure 3A, condition B). When the Mn^{2+} ions were added both inside and outside the vesicles, all of the DMPC headgroup resonances were completely broadened, as expected (Figure 3A, condition C). Addition of EDTA to DMPC vesicles containing Mn^{2+} both inside and outside regenerated all of the headgroup resonances from the outer monolayer (Figure 3A, condition D).

Unlike DMPC, only one resonance for each chemical group was obtained for sonicated AC2 dispersions (Figure 3B (condition A) and Table 1). Addition of Mn^{2+} to the AC2 dispersion (condition B) caused broadening of all of the resonances from the AC2 headgroup, including (i) the two adjacent methylene groups in the choline headgroup (δ 3.700 and 4.320 ppm), (ii) the glycerol methine proton (δ 5.300 ppm), and (iii) the choline *N*-methyls (δ 3.275 ppm). In addition, there was no difference in the ^{1}H NMR spectra of AC2 when the Mn^{2+} ion was merely added to the AC2 sonicated dispersion compared to when the Mn^{2+} ion was present during sonication of the AC2 lipid (compare Figure 3B condition B with condition C). Addition of EDTA to AC2 lipid dispersions containing Mn^{2+} caused the previously broadened signals to reappear (Figure 3B, condition D). These results clearly demonstrate that all of the AC2 lipid molecules in sonicated dispersions are accessible to the bulk aqueous medium. In other words, the AC2 lipid particles formed by sonication do not have an inner monolayer of lipid as found in SUVs. This is consistent with the observation that these particles would not entrap Dextran-4000. Lack of entrapment indicates that the particles are micelle structures.

The ether *O*-methyl protons located at the terminal part of the acyl chains of the AC2 molecule were not broadened by the Mn^{2+} ions. Both of the ether *O*-methyls exhibit a narrow resonance at 3.3 ppm in the presence (condition B) and absence (condition C) of Mn^{2+} ions (Figure 3B). The inaccessibility of the ether *O*-methyl to an Mn^{2+} broadening effect indicates that the terminal *O*-methyl group remains in a hydrophobic environment on the NMR time scale. Terminal methyls from interdigitated acyl chains would be accessible to Mn^{2+}, and the lack of accessibility to Mn^{2+} eliminates the possibility that sonicated AC2 lipid dispersions form an interdigitated phase. ^{1}H NOESY spectroscopy discussed below corroborates these results.

Figure 4 compares Arrhenius plots of T_1 vs temperature for both DMPC and AC2 sonicated lipid dispersions. For both

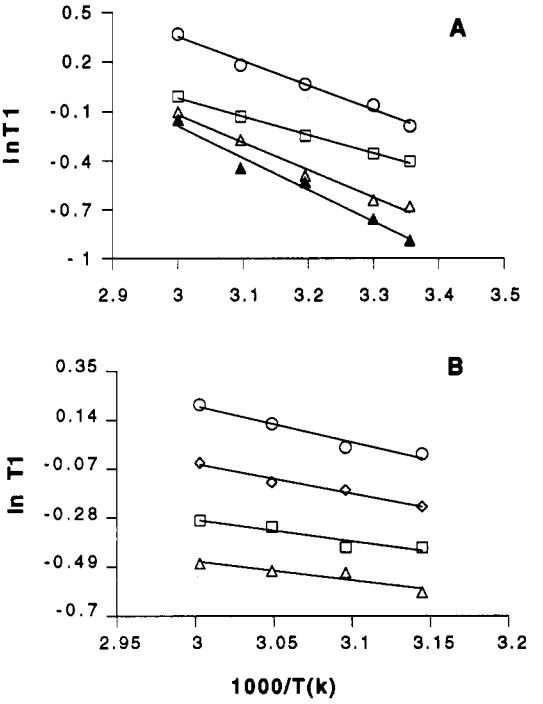

FIGURE 4: Temperature dependence of the ^{1}H T_1 relaxation times at 500 MHz for sonicated DMPC (A) and AC2 (B) dispersions. Representative functional groups are ω-CH_3 or OCH_3 (○), OCH_2 (◇), $(CH_2)_n$ (□), outer $N(CH_3)_3$ (△), and inner $N(CH_3)_3$ (▲). The solid lines were calculated by linear regression, and the r^2 coefficients are listed in Table 2.

Table 2: Motional Activation Energies (E_a) of DMPC and AC2 in Sonicated Lipid Dispersions

functional groups	E_a (kcal/mol) DMPC	AC2
ω-CH_3	2.90[a] (r^2 = 0.988)	
OCH_3		3.08 (r^2 = 0.957)
OCH_2		2.52 (r^2 = 0.975)
$(CH_2)_n$	2.20[a] (r^2 = 0.996)	1.80 (r^2 = 0.881)
$N(CH_3)_3$	3.36 (outer, r^2 = 0.983)	1.61 (r^2 = 0.862)
	3.90 (inner, r^2 = 0.976)	

[a] We note that the inner and outer monolayers of DMPC SUVs contain $(CH_2)_n$ and ω-CH_3 groups, and the E_a values are the averages of these two environments.

DMPC and AC2, four well-resolved resonances were analyzed for Arrhenius behavior: (i) the terminal methyl group; (ii) the methylene envelope; (iii) headgroup choline *N*-methyls in the inner monolayer; and (iv) choline *N*-methyls in the outer monolayer. However, since the *O*-methylene group in the AC2 molecule was well resolved, it was also included in the T_1 analysis. Motional activation energies (E_a's) obtained from the slopes of the T_1 vs temperature plots are summarized in Table 2 for each chemical group.

The E_a of the choline *N*-methyl protons is higher for the inner monolayer compared to the outer monolayer (3.90 vs 3.36 kcal/mol) for DMPC SUVs (Figure 4A and Table 2). This indicates that the choline *N*-methyl groups forming the inner monolayer are motionally restricted in comparison to the outer monolayer choline *N*-methyls; the negative curvature of the inner monolayer (Seddon, 1990) causes tighter packing of the polar headgroups in SUVs. In addition, the E_a's of the methylene envelope ($(CH_2)_n$) and the terminal methyl group (ω-CH_3) are lower than the E_a's of both the inner and outer choline *N*-methyls (*N*-CH_3) of DMPC SUVs (Table 2). This indicates that the DMPC hydrocarbon chains are loosely packed compared to the DMPC headgroup regions in SUVs;

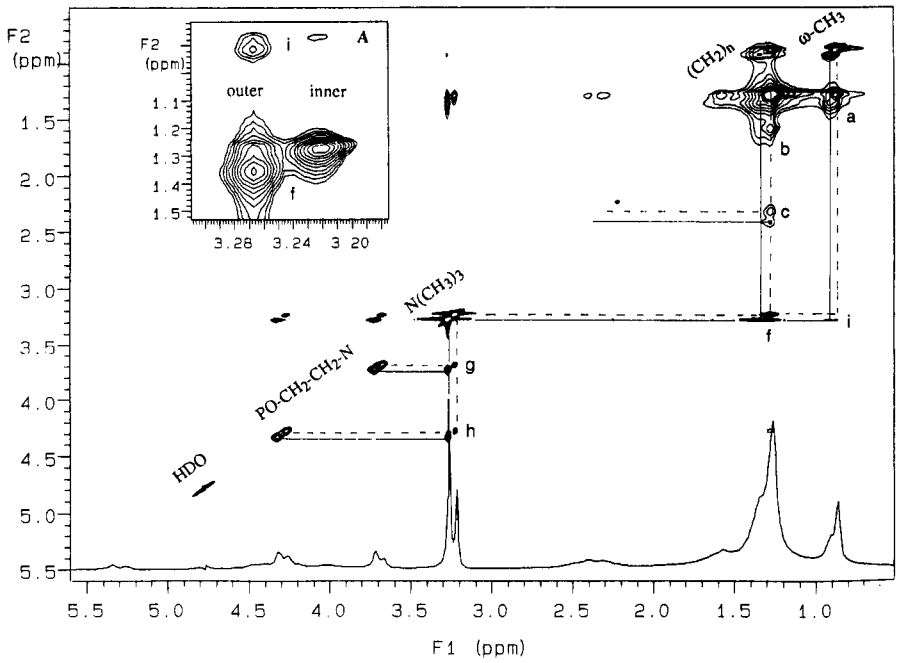

FIGURE 5: 500-MHz ^{1}H pure absorption phase NOESY spectrum of sonicated DMPC lipid dispersions obtained at 25 °C with a mixing time of 300 ms. The chemical groups are labeled along their diagonal peaks, and the cross peaks are labeled with single lower case letters. The NOE dipolar connectivities from the outer monolayer of lipids are indicated with solid lines, and those from the inner monolayer are indicated with dashed lines. A 1D spectrum is shown on the bottom of the 2D NOESY contour plot.

these results are consistent with previous studies of DMPC and DPPC MLVs in the L_α phase (Fobes et al., 1988; Halladay et al., 1990).

Choline *N*-methyls of AC2 have an E_a of 1.61 kcal/mol, which is less than one-half the E_a for the choline *N*-methyls of DMPC (Table 2). This lower motional activation energy indicates that the headgroup motion of AC2 molecules in AC2 lipid aggregates prepared by sonication is less restrained compared to DMPC molecules in SUVs. More interesting, there is a trend showing that E_a increases from the headgroup choline *N*-methyl region to the end of the acyl chains for AC2 molecules (Table 2). This motional activation energy gradient is consistent with spherical or cylindrical micelle structures that are expected to have very loose packing at the polar interface (low E_a) and tighter packing in the micelle core (high E_a). Although the AC2 micelles may be either spherical or cylindrical, the TEMs indicate that the micelles are spherical (Figure 2).

The segmental motion of the acyl chains in AC2 micelles was studied further using two-dimensional nuclear Overhauser effect experiments (NOESY). NOESY experiments provide structural and dynamic information about lipid molecules assembled as bilayer vesicles, micelles, or interdigitated bilayers (Ellena et al., 1985; Xu & Cafiso, 1986; Stark et al., 1986; Gabriel & Roberts 1987; Halladay et al., 1990; Jonas et al., 1990). Double diagonal peaks exist in the NOESY spectra of DMPC (Figure 5 and Table 3). These doublets correspond to the inner and outer monolayer lipids of DMPC SUVs. Tighter packing of lipid molecules causes all of the proton resonances to shift to high field, and the doublets are a direct indication of the differences in lipid packing between the inner and outer lipid monolayers (Schuh et al., 1982; Xu & Cafiso, 1986). Lipid packing differences between the inner and outer lipid monolayers were also apparent in the cross peaks of the NOESY spectrum (Figure 5). Scaling the cross-peak volumes relative to the corresponding diagonal peak volumes (Macura et al., 1986) reveals that cross-relaxation is 1.8 times more efficient for $N(CH_3)_3/(CH_2)_n$ interactions on the inner monolayer compared to the outer monolayer.

Table 3: Proton Dipolar Connectivities from the NOESY Data of Sonicated Lipid Dispersions

cross peak[a]	dipolar connectivity	DMPC	AC2
a	$(CH_2)_n$–CH_3	x	
a′	$(CH_2)_n$–OCH_3		x
b	$(CH_2)_n$–CH_2CH_2CO	x	x[b]
b′	$(CH_2)_n$–CH_2CH_2O		x[b]
c	$(CH_2)_n$–CH_2CO	x	x
d	$(CH_2)_n$–OCH_2		x
e	CH_2OCH_3		x
f	$N(CH_3)_3$–$(CH_2)_n$	x	x
g	CH_2–$N(CH_3)_3$	x	x
h	$POCH_2CH_2N(CH_3)_3$	x	weak
i	$N(CH_3)_3$–CH_3	weak	
l	$CH_2CH_2OCH_3$		x
m	CH_2CH_2O		x

[a] Cross peaks are from the NOESY spectra for DMPC and AC2 (Figures 5 and 6). [b] The resonances for the CH_2CH_2CO group (located near the interfacial region) overlap with those for the CH_2CH_2O group (located in the hydrophobic region) in AC2 lipid dispersions. This dipolar connectivity can therefore result from either group.

However, ω-$CH_3/(CH_2)_n$ interactions are only 0.3 times as efficient on the inner monolayer compared to the outer monolayer of DMPC SUVs. These results are consistent with the results reported from Cafiso's group (Ellena et al., 1985; Xu & Cafiso, 1986) and indicate a packing asymmetry between the lipids within the inner and outer monolayers of SUVs.

In general, more efficient cross-relaxation occurs for functional groups that are more closely packed, and the NOESY data is consistent with this view. The polar headgroups of phospholipids forming the inner monolayer surface are packed closer than the same functional groups forming the outer monolayer surface of SUVs, which is in agreement with the 1.8 times more efficient cross-relaxation for $N(CH_3)_3/(CH_2)_n$ interactions. Regarding the acyl chain packing differences, the nonpolar acyl chains pack loosely in the inner monolayer compared to the outer monolayer, which is consistent with weak ω-$CH_3/(CH_2)_n$ interactions causing weak cross-relaxation between these groups in the inner monolayer. The nature of the packing differences between

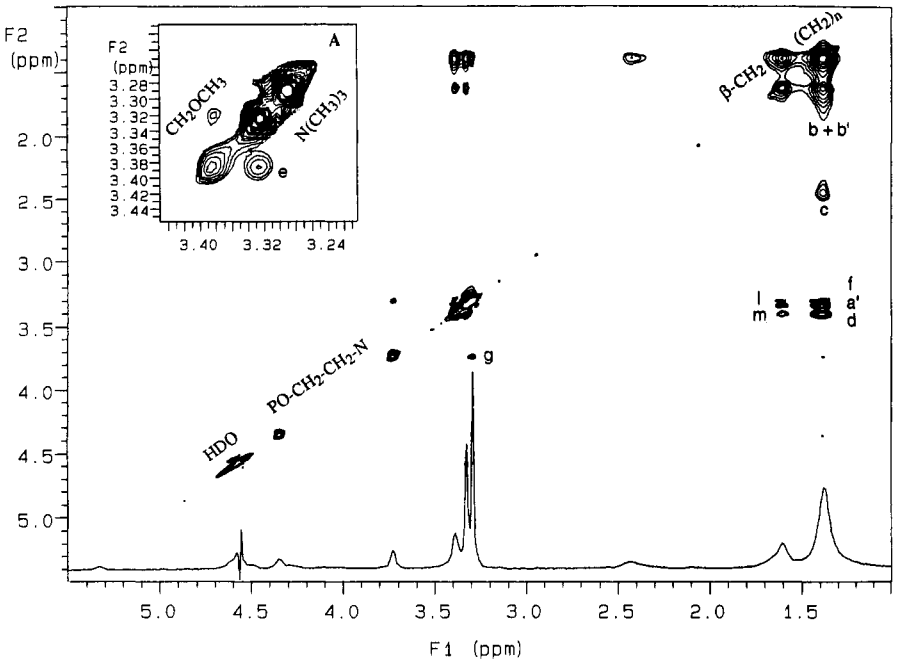

FIGURE 6: 500-MHz ^{1}H pure absorption phase NOESY spectrum of sonicated AC2 lipid dispersions obtained at 50 °C with a mixing time of 300 ms. The chemical groups are labeled along their diagonal peaks, and the cross-peaks are labeled with single lower case letters. A 1D spectrum is shown on the bottom of the 2D NOESY contour plot. Inset A is an expanded plot of diagonal peaks and cross peaks in the choline headgroup $N(CH_3)_3$ region.

the inner and outer monolayers of lipid in these SUVs has been described previously on the basis of ^{31}P NMR and hydrodynamic data (Huang & Mason, 1978), statistical lattice theory (Dill & Flory, 1981), and ^{1}H NMR studies (Schuh et al., 1982).

The NOESY spectra of sonicated AC2 dispersions show only a single resonance for the diagonal peaks, and each functional group of the AC2 molecule exhibits only one cross peak, i.e., only one dipolar connectivity (Figure 6). There is also no cross peak between the choline *N*-methyls in the polar headgroup region and the ether *O*-methyls at the terminal part of the lipid acyl chains (see the insert in Figure 6). The lack of dipolar connectivity between these two groups supports the hypothesis that AC2 sonicated lipid particles do not have interdigitated chains.

Because of fast molecular motion on the NMR time scale ($\tau_c\omega_o \ll 1$), conventional short-chain (<8 carbons) diacylated phospholipid micelles do not exhibit positive cross peaks concurrently with positive diagonal peaks in the NOESY spectra at any mixing time (Stark et al., 1986; Gabriel & Roberts, 1987). However, the NOESY spectrum of AC2 micelles (Figure 6) shows all positive cross peaks in the hydrocarbon chain region, which is similar to the cross peaks observed in the NOESY spectra of DMPC SUVs (Table 3). Thus, the segmental hydrocarbon chain motions of AC2 in the micelles are in the slow motion regime ($\tau_c\omega_o \gg 1$), which is similar to the segmental hydrocarbon chain motions of DMPC in bilayer vesicles. Cross-peak h, between the choline *N*-methyl and *O*-methylene groups, in the NOESY spectrum of DMPC (Figure 5) is absent from the spectra of AC2 dispersions (Figure 6). This indicates faster segmental headgroup motions of AC2 molecules in micelles compared to the same lipid headgroup in DMPC SUVs. NOESY data thus corroborate the conclusions based on the motional activation energies E_a (obtained from ^{1}H T_1 measurements), which showed that the headgroup motions of AC2 in the micelles are less hindered compared to the headgroup motion of DMPC in bilayer vesicles.

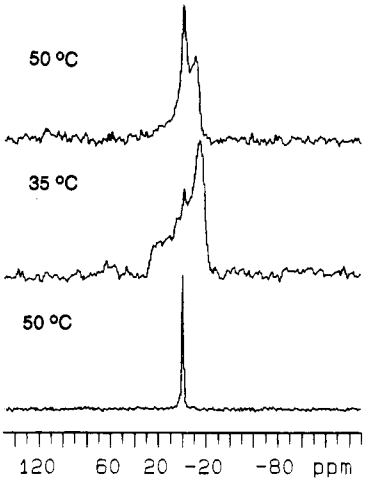

FIGURE 7: 202-MHz ^{31}P NMR spectra of sonicated AC2 lipid dispersions above and below the T_m. The lower spectrum corresponds to an AC2 dispersion that was sonicated above T_m and maintained above T_m prior to insertion into the NMR spectrometer, with the probe preequilibrated to 50 °C. NMR parameters for data acquisition are given in the legend for Figure 2. The middle spectrum corresponds to the sonicated AC2 dispersion that was cooled from 50 to 35 °C outside the magnetic field; the middle spectrum was obtained at 35 °C using a 0.1-s acquisition time, 950 transients, and a 300-Hz line-broadening function. The upper spectrum corresponds to reheating the sample from the middle spectrum from 35 to 50 °C. Data acquisition parameters for the upper spectrum were a 0.2-s acquisition time, 750 transients, and a 200-Hz line-broadening function.

AC2 micelles fuse extensively as the temperature is reduced from above the main transition temperature (T_m) to below T_m of the lipid. This fusion event was monitored by both ^{31}P NMR spectroscopy and TEM (Figures 7 and 8). Sonicated dispersions of AC2 exhibit an isotropic ^{31}P NMR line shape with $\Delta\nu_{1/2}$ = 0.8 ppm. When the sonicated AC2 lipid dispersions are then cooled from 50 to 35 °C outside the NMR spectrometer in a water bath for 10 min, the resulting ^{31}P NMR spectrum obtained at 35 °C is an axially symmetric powder pattern with a low-intensity shoulder ($\sigma_\parallel$) at 26.0 ppm,

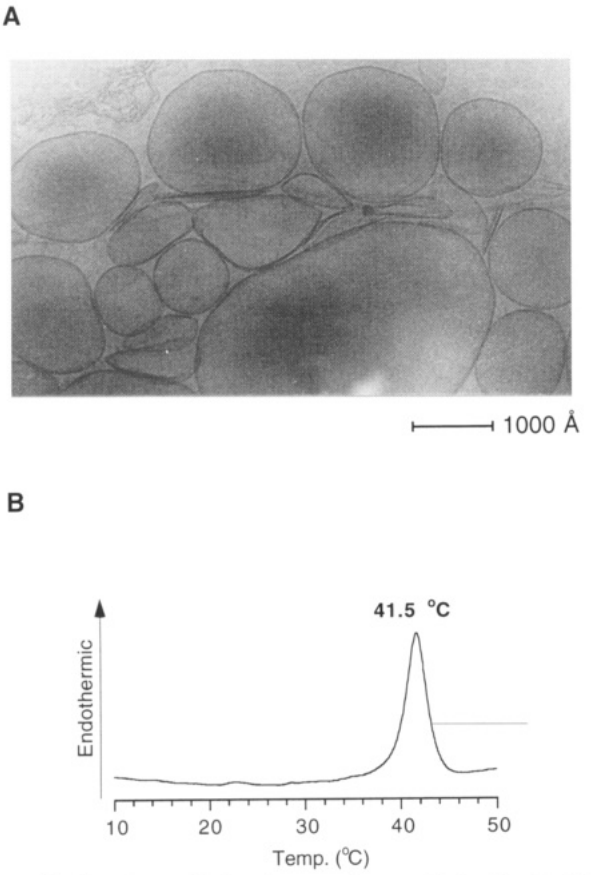

FIGURE 8: Cryo-transmission electron micrograph showing the lipid structures formed by the fusion of AC2 micelles. Fusion was initiated by reducing the temperature from above the T_m (50 °C) to 35 °C. The DSC thermogram obtained from AC2 liposomes formed by AC2 micelle fusion is given.

a high-intensity shoulder ($\sigma_\perp$) at −13.0 ppm, and a spectral breadth ($\Delta\sigma$) of 39.0 ppm (Figure 7, middle spectrum). This dramatic line shape change from the isotropic resonance at 0 ppm (Figure 7, bottom spectrum) to the axially symmetric powder pattern below T_m (Figure 7, middle spectrum) clearly indicates that small AC2 micelles fuse into large lipid structures when the temperature is reduced from above T_m to below T_m. When the sample was reheated in the NMR spectrometer from 35 to 50 °C, an isotropic resonance at 0 ppm was superimposed on the axially symmetric powder pattern; the spectral features of the axially symmetric powder pattern are $\sigma_\parallel = 24.0$ ppm and $\sigma_\perp = -10.0$ ppm (Figure 7, upper spectrum). The isotropic component is broader ($\Delta\nu_{1/2} = 10$ ppm) than the isotropic resonance from the initial AC2 micelle structures ($\Delta\nu_{1/2} = 0.8$ ppm) (bottom spectrum). On the basis of the ~10-fold increase in the ^{31}P NMR line width of the isotropic component in the reheated sample, the particles are most likely small liposomes and not micelles. In addition, a high-resolution ^{1}H NMR spectrum could not be obtained from the reheated sample. This result further supports that AC2 lipid particles in the reheated sample are no longer AC2 micelles, but rather they are small bilayer vesicles in the diameter range 1000–1500 Å. This liposome size will generate an isotropic ^{31}P NMR resonance with a line width that is similar to the line width shown for the isotropic component in Figure 7 (upper spectrum).

Multilayered liposomes and large single-layered liposomes do not give well-resolved ^{1}H NMR spectra because the lipid particles are large; only small SUVs and micelles give well-resolved ^{1}H NMR spectra. A high-resolution ^{1}H NMR spectrum was obtained for sonicated AC2 lipid dispersion prepared and maintained at 50 °C (Figure 3B, condition A). However, if the sample was cooled below T_m and then reheated above the T_m, a featureless ^{1}H NMR spectrum was obtained. Thus, increasing the temperature will not convert the large fused AC2 particles back into small micelle structures; sonication is needed to form the AC2 micelles.

Large AC2 structures were confirmed visually by cryo-TEM micrographs (Figure 8). Cryo-TEM micrographs of AC2 show that fusion causes the formation of large spherical particles with diameters in the range 1000–5000 Å (Figure 8). When Dextran-4000 was added prior to fusion, the AC2 liposomes that formed by fusion entrapped large amounts of Dextran-4000; the encapsulation efficiency was ~4 μL/μmol of lipid. Thus, the large AC2 liposomes contain a large aqueous compartment, and cryo-TEM micrographs show only large unilamellar vesicles. Furthermore, the liposomes formed from the fusion of AC2 micelles undergo the same endothermic transition of AC2 MLVs formed without sonication (compare the thermogram in Figure 8 to that in Figure 1). This indicates that the lipid molecular packing in the liposomes formed by AC2 micelle fusion is identical to that in AC2 MLVs.

Unlike the AC2 discussed above, the size of DMPC SUVs did not change when they were cooled below T_m. This is based on ^{31}P NMR spectra of sonicated DMPC dispersions that show a narrow symmetric line shape near 0 ppm both at 30 °C and when cooled to 18 °C (compare Figure 2 to Figure 9); heating and cooling did not affect either the line shape or the chemical shift, but $\Delta\nu_{1/2}$ increased from 0.8 ppm (above T_m) to 1.5 ppm (below T_m). The TEMs of sonicated DMPC dispersions obtained above and below the T_m also showed no significant change in vesicle size (compare Figure 2 to Figure

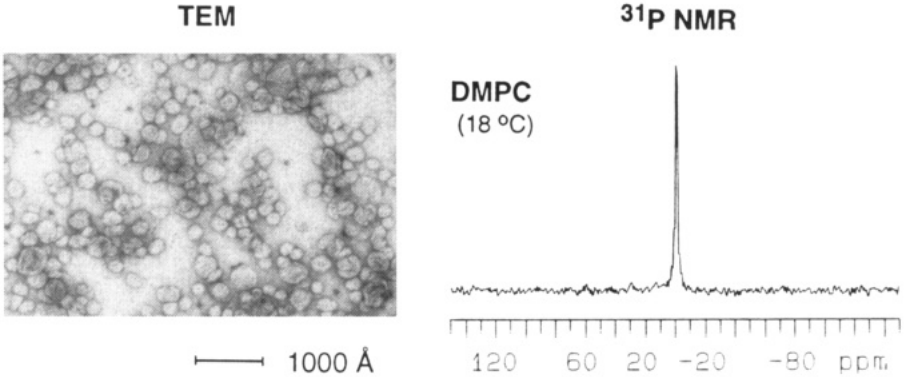

FIGURE 9: Negative-stain electron micrograph and 202-MHz ^{31}P NMR spectrum of sonicated DMPC lipid dispersions below the T_m. The DMPC spectrum was obtained at 18 °C using an acquisition time of 0.2 s, and 300 transients were signal-averaged. Prior to Fourier transformation a 100-Hz line-broadening function was used.

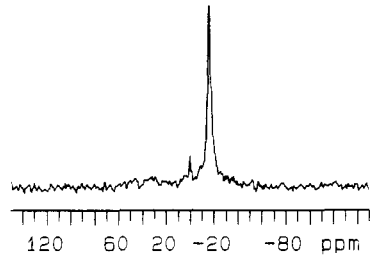

FIGURE 10: Fusion of AC2 membranes in the magnetic field of NMR spectrometers causes orientation of the large fused-membrane structures. The spectral intensity at the perpendicular edge of the spectrum indicates that the AC2 membranes are oriented with the long axis of the lipid molecules perpendicular to the magnetic field direction. The sample used to obtained the ^{31}P NMR spectrum in Figure 7 was cooled from 50 to 35 °C inside the NMR spectrometer, and the spectrum was obtained using the same data acquisition parameters.

9). Therefore, the SUV formed from DMPC does not exhibit temperature-dependent fusion like that from AC2. Although it has been reported previously that SUVs formed from DPPC, DSPC, and DAPC grow in size when incubated below the T_m's of each lipid (Schullery et al., 1980; Nayar et al., 1989), the actual size increase is modest compared to the size increase of the fused AC2 micelles. For instance, vesicles with diameters of about 700 Å were observed after incubating DPPC SUVs at 21 °C (20 °C below the T_m of DPPC) for 9 days (Schullery et al., 1980). AC2 micelles of ~70 Å are converted into 1000–5000-Å liposomes in seconds when the temperature is reduced from above to below the T_m of AC2.

The typical axially symmetric powder pattern shown in Figure 7 (middle spectrum) was obtained from sonicated AC2 dispersions that were cooled from 50 to 35 °C *outside* the NMR spectrometer. When the AC2 lipid dispersion is cooled *in* the NMR spectrometer (11.7 T), the ^{31}P NMR spectrum shows some evidence of an axially symmetric powder pattern with $\sigma_\parallel \approx 33.0$ ppm and $\sigma_\perp = -16.0$ ppm, but most of the spectral intensity is at the perpendicular edge of the spectrum ($\sigma_\perp$) (Figure 10). This distorted line shape is due to magnetically induced orientation of the lipid (Qiu et al., 1993). Our earlier studies of the magnetically induced orientation of lipid membranes demonstrated that, although all bilayer vesicles can be oriented to some extent in high magnetic fields (i.e., 11.7 T), only large liposomes (>5 μm) will quantitatively orient at this magnetic field strength. The key concept is that both micelle and small unilamellar vesicles are not susceptible to magnetically induced orientation. Thus, the line shape change associated with fusion in the magnetic field, which involves the conversion of an isotropic line to a spectrum with enhanced intensity at $\sigma_\perp$, indicates that the magnetic field promotes the fusion of AC2 micelles into giant lipid sheets that orient parallel to the magnetic field with respect to the bilayer. In other words, the field participated in the fusion event by increasing the size of the lipid structures formed by fusion.

The stability of AC2 micelles when the temperature is maintained above the T_m, is shown in Figure 11; no change in the ^{31}P NMR line shape occurred over 96 h, indicating that little if any change occurred in the micelle structure during this 4-day incubation at 50 °C. However, when the temperature was reduced to 35 °C for only 4 h, the line shape was converted from an isotropic line shape into an axially symmetric powder pattern (Figure 11, inset), which is indicative of the formation of large liposomes. These results suggest that it is not the time that determines the stability of AC2 micelles, rather it is the temperature: reduction of the temperature of sonicated AC2 dispersions to below the T_m of AC2 causes a micelle-to-bilayer transition.

DISCUSSION

Scheme 1 compares the physicochemical properties of DMPC (upper diagram) to those of AC2 (lower diagram). Although both phospholipids have a similar acyl chain length, sonication above T_m of DMPC results in SUVs, whereas sonication of AC2 above T_m results in micelles. DMPC SUVs

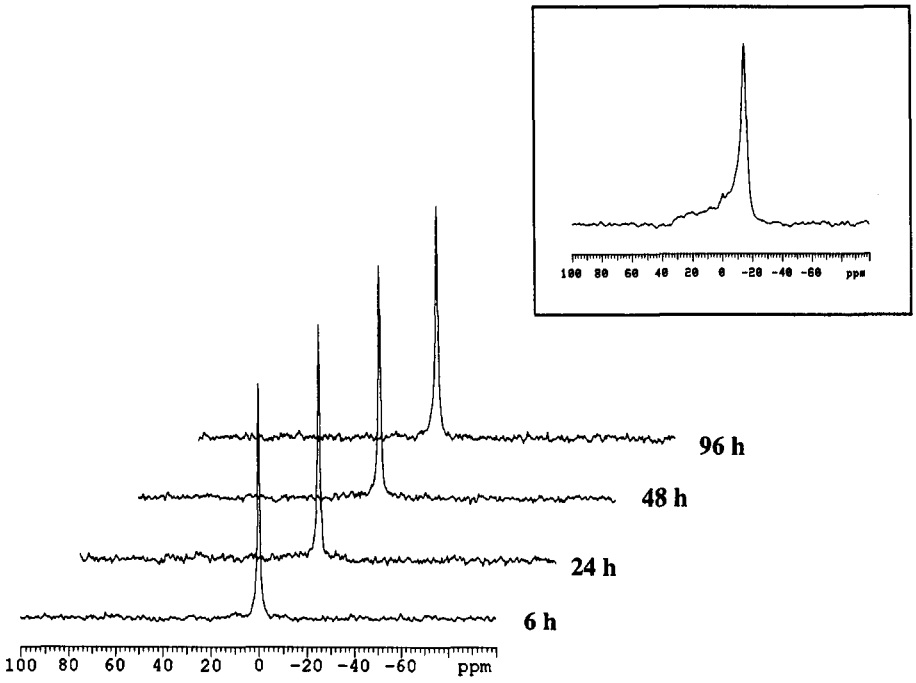

FIGURE 11: ^{31}P NMR spectra of sonicated AC2 dispersions maintained at 50 °C over a 96-h incubation period. NMR data acquisition parameters are given in the legend to Figure 2. The inset shows the ^{31}P NMR spectrum of the AC2 dispersion after the temperature was changed from 50 to 35 °C. NMR data acquisition parameters for the powder pattern shown in the inset are given in the legend to Figure 7. On the basis of TLC analysis, no degradation of the AC2 phospholipid occurred during the 96-h incubation.

Scheme 1: Diagram Comparing the Membrane Properties of DMPC to AC2 Dispersions

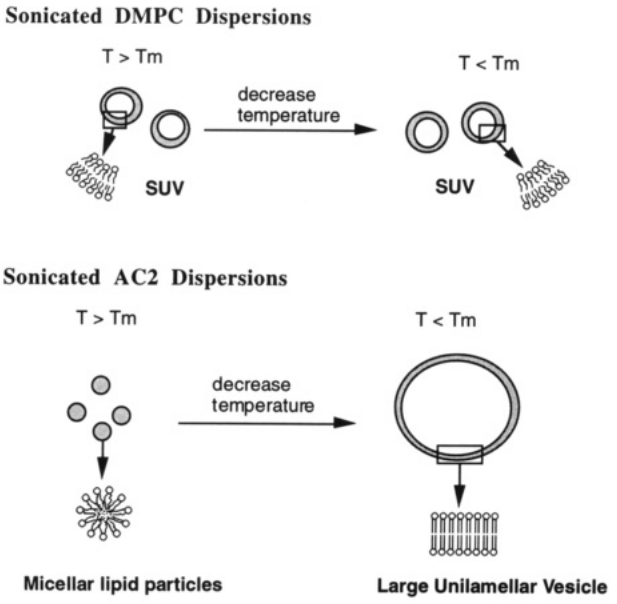

are thermodynamically stable, and consequently, the vesicles remain intact without a temperature-induced size change (Scheme 1, upper diagram). In contrast, AC2 micelle structures are unstable at temperatures near T_m. As depicted in Scheme 1, when the temperature is reduced below the T_m of AC2, the micelles convert into large liposomes (Scheme 1, lower diagram). The large AC2 liposomes entrap Dextran-4000 and are single-layered with a high encapsulation efficiency ($\sim$4 μL/μmol).

Below T_m, the acyl chains of DMPC and most likely AC2 adopt an all-trans conformation that increases the acyl chain packing density. However, since the T_m of AC2 is 18 °C higher than the T_m of DMPC, and the ΔH of AC2 is 2 kcal/mol higher than that of DMPC, more thermal energy is needed to melt the acyl chains of AC2 compared to DMPC. This indicates that AC2 molecules are packed tighter than DMPC molecules below the T_m. On the basis of DSC studies that Menger's group performed on diacylated phospholipids containing ketones in both of the phospholipid acyl chains (Menger et al., 1988), we believe that the tighter lipid packing below T_m is caused by dipole–dipole interactions from the adjacent ether atoms near the center of the bilayer, and this is currently under investigation.

Bilayer formation by the sonication of aqueous DMPC dispersions is well understood, but micelle formation by the sonication of AC2 dispersions was not expected. Sonication disrupts multilamellar liposomes by tearing them into small bilayer fragments (Finer et al., 1972; Pidgeon et al., 1986, 1987). For long-chain diacylated phospholipids (>12 carbons/chain), the bilayer fragments are thermodynamically unstable intermediates that minimize their membrane edge energy by forming small closed membrane structures denoted as vesicles (Lasic, 1988; Helfrich, 1974). The membrane edge energy of bilayer fragments arises from the partial contact between the water and the hydrocarbon chains of the phospholipid (Lipowsky, 1991). In other words, the hydrophobic effect is the driving force for the bilayer fragments to assemble into closed vesicles.

AC2 is a chemical analog of DMPC that contains an oxygen atom substituted for each C13 methylene group in the lipid acyl chains (Figure 1). For free fatty acids, this oxygen-for-methylene substitution causes a decrease in the hydrophobicity equivalent to removing $\sim$2–4 carbon atoms from the fatty acid (Heuckeroth et al., 1988). Thus, AC2 with two fatty acid chains is expected to be significantly less hydrophobic than DMPC. This reduced hydrophobicity lowers the edge energy of AC2 bilayer fragments generated by the sonication of multilayered AC2 liposomes. The edge energy associated with small AC2 bilayer fragments is much less than the edge energy of DMPC bilayer fragments. Consequently, AC2 molecules in the lipid particles formed by sonication either (i) do not form bilayer fragments and organize into a micelle structure or (ii) form bilayer fragments that reorganize into a micelle structure to minimize their edge energy. Although the hydrophobicity of AC2 is less than that of DMPC, it is higher than those of short-chain phospholipids (<8 carbons/chain). This intermediate hydrophobicity (less than long-chain phospholipids, but greater than short-chain phospholipids) of a molecule with a long acyl chain length inhibits AC2 molecules from spontaneously forming micelles as do short-chain phospholipids; mechanical energy (i.e., sonication) is required to tear the AC2 multilamellar liposomes into membrane fragments that ultimately become AC2 micelles.

Micelles prepared from short-chain phospholipids are thermodynamically stable, and these short-chain phospholipids have molecular geometries and hydrophobicities that are predicted to form micelle structures on the basis of Israelachvilli's model (Israelachvilli & Mitchell, 1975). AC2 micelles are not thermodynamically stable because the replacement of methylene for oxygen significantly reduces the hydrophobicity of AC2; however, the acyl chain length of AC2 phospholipids remains virtually unchanged (Heuckeroth et al., 1988). In other words, although the hydrophobicity of AC2 is similar to those of phospholipids with diacyl chains containing 10–12 carbons, the geometry of the AC2 molecule is similar to that of DMPC (14 carbons/chain), which is cylindrical in shape (de Kruijff et al., 1975). Pure DMPC aqueous dispersions cannot form micelles under any condition, whereas AC2 spontaneously formed micelles when sonicated above the T_m. Above the T_m the geometry of the AC2 molecule cannot be purely cylindrical or micelles could not form. Consequently, above the T_m of the lipids, the acyl chain trans:gauche population ratio of AC2 must significantly differ from that of DMPC, and the acyl chain conformation must allow for micelle formation.

In addition, the trans:gauche population of AC2 above the T_m significantly changed the area/molecule of AC2 molecules in the micelle structure. The increase in the AC2 area/molecule is based on both the T_1 data used to calculate the motional activation energy (Figure 4 and Table 2) and NOESY experiments (Figures 5 and 6), which clearly showed that the headgroup motions of AC2 molecules in their micelle structures are less restrained than the headgroup motion of DMPC molecules in SUVs. This less hindered headgroup motion indicates that AC2 micelles have an interfacial area/molecule greater than that of DMPC SUVs, as depicted in Scheme 1. Consequently, more hydrophobic methylene groups become exposed to the aqueous phase, so that the micelle surface becomes more hydrophobic, which contributes to the instability of the AC2 micelles. Interfacial hydrophobicity has been suggested to be the main driving force for membrane fusion (Ohki, 1982; Helm et al., 1992). Thus, the exposed hydrocarbon at the AC2 micelle surface increases the tendency of AC2 micelles to fuse. In addition to hydrophobicity, conformational changes in the AC2 acyl chains play an important role in the fusion of AC2 micelles.

The fusion of AC2 micelles occurs at the main transition temperature, and therefore the macroscopic fusion of AC2 particles (~70 Å) into large liposomes must depend on molecular changes associated with the main transition temperature of AC2. Reducing the temperature from above to below the T_m reduces the conformational freedom of the acyl chains; a significant reduction in the interconversion rate of trans to gauche conformers occurs. In other words, below T_m the acyl chains tend to adopt a "straight"-chain conformation, and the rate of interconversion of the trans/gauche conformers is reduced. In bilayers, molecular packing constraints usually become more pronounced when the temperature is reduced below the main transition temperature of the phospholipid, and straight acyl chains must pack to form the membrane (Schullery et al., 1980; Helm et al., 1992). For AC2 micelles, the molecular packing constraints also increase when the temperature is reduced below the T_m and acyl chains are in an all-trans conformation; this conformation forces the AC2 molecule to adopt a cylindrical geometry similar to DMPC, and micelles cannot exist with this geometry. Thus, when the AC2 acyl chains adopt the all-trans conformation, the AC2 micelle structure must either (i) fuse with neighboring micelles to form liposomes or (ii) convert into bilayer fragments.

The AC2 bilayer fragment, with exposed hydrocarbon chains, exhibits high edge energy (Lipowsky, 1991). Fusion or self-assembly of the AC2 bilayer fragments spontaneously occurs to eliminate the high edge energy. Because membrane edge energy is proportional to the linear size of the bilayer fragment whereas the curvature energy is not (Lipowsky, 1991; Helfrich, 1974), the membrane edge energy of large fused AC2 bilayer fragments eventually will be large enough to overcome the curvature elasticity to form closed bilayer liposomes; closed bilayer liposomes were clearly shown by ^{31}P NMR spectra (powder pattern in Figure 7, middle spectrum), TEM micrographs (Figure 8), and Dextran-4000 trapping experiments. In addition, the large liposomes formed by the fusion of AC2 micelles exhibit a main phase transition with the same T_m as that of AC2 MLVs. Thus, the acyl chains of AC2 molecules adopt the all-trans conformation below the T_m, regardless of the method used to assemble the lipids into bilayer structures.

The fusion of AC2 liposomes in the magnetic field of a ^1H 500-MHz spectrometer resulted in larger liposomes (Figure 10 is the ^{31}P NMR spectrum; TEMs are not shown) compared to when fusion was performed outside the magnetic field (Figure 7). The magnetic field thus influences the fusion event. In a magnetic field, the preferred orientation for phospholipid bilayer membranes occurs when the membrane surface is parallel to the magnetic field (Qiu et al., 1993). Several phospholipid membranes quantitatively orient their membranes in the 11.7-T field of ^1H 500-MHz spectrometers. Magnetically induced orientation depends on both the fluidity of the membrane and the size of the liposomes (Qiu et al., 1993). For small vesicles and liposomes, thermal energy (responsible for rapid tumbling and reorientation of the lipid particles) is greater than the magnetic orientation force, but for large liposomes the magnetic orientation energy on the lipid structure is greater than the thermal energy. The magnetic force of modern NMR spectrometers is sufficient to distort spherical liposomes into elliptical structures (Qiu et al., 1993; Brumm et al., 1992; Reinl et al., 1992). When AC2 micelles fuse in the magnetic field, the magnetic energy most likely stabilizes the large fused bilayer fragments and orients the membranes parallel to the magnetic field.

The two phospholipid monolayers forming the DMPC SUV membrane are intrinsically asymmetric; the inner and outer bilayer surfaces have quite different surface curvatures both in magnitude and in sign (Seddon, 1990). The outer monolayer surface adopts positive curvature (i.e., curving toward the hydrocarbon chain region) and the inner monolayer adopts negative curvature (i.e., curving toward the aqueous exterior). In addition, the inner monolayer has higher curvature than the outer monolayer. However, spherical or cylindrical micelles only have surfaces with positive curvature. Consequently, micelle formation of sonicated AC2 dispersions suggests that AC2 lipids cannot form surfaces with the small negative curvature that is required for the formation of SUVs. Structures with small negative curvature have been hypothesized to be on the biochemical pathway of membrane fusion (Siegel, 1987; Siegel et al., 1989). In addition, it has been reported that the mechanism of inhibition of viral and cell membrane fusion by small hydrophobic peptides is due to their destabilization of membrane structures with a small negative curvature (Yeagle et al., 1992). Similarly, the antiviral activity of AC2 may be related to the inability of AC2 surfaces to form structures with a small negative membrane curvature that would be found on the inner membrane of an HIV virus that is budding from a host cell.

ACKNOWLEDGMENT

We are very grateful to Debby Sherman for obtaining the negative-stain electron micrographs and Dr. Timothy Baker and G. J. Wang for obtaining cryo-TEMs of AC2 (Dr. Baker is supported by NIH Grant GM33050, G. J. Wang is supported by the Lucile T. Markey Charitable Trust at the Purdue Structural Biology Center).

REFERENCES

Bian, J., & Roberts, M. F. (1990) *Biochemistry 29*, 7928–7935.
Brumm, T, Mops, A., Dolainsky, C., Bruckner, S., & Bayer, T. M. (1992) *Biophys. J. 61*, 1018–1024.
Bryant, M. L., Heukeroth, R. O., Kimata, J. T., Ratner, L., & Gordon, J. I. (1989) *Proc. Natl. Acad. Sci. U.S.A. 86*, 8655–8659.
Bryant, M. L., Ratner, L., Duronio, R. J., Kishore, N. S., Devadas, B., Adams, S. P., & Gordon, J. I. (1991) *Proc. Natl. Acad. Sci. U.S.A. 88*, 2055–2059.
Burnell, E. E., Cullis, P. R., & de Kruijff, B. (1980) *Biochim. Biophys. Acta 603*, 63–69.
Cullis, P. R., & de Kruijff, B. (1979) *Biochim. Biophys. Acta 559*, 399–420.
DeBose, C. D., & Roberts, M. F. (1983) *J. Biol. Chem. 258*, 6327–6334.
de Kruijff, B., Cullis, P. R., & Radda, G. K. (1975) *Biochim. Biophys. Acta 406*, 6–20.
Dill, K. A., & Flory, P. (1981) *Proc. Natl. Acad. Sci. U.S.A. 78*, 3676–680.
Ellena, J. F., Hutton, W. C., & Cafiso, D. S. (1985) *J. Am. Chem. Soc. 107*, 1530–1537.
El-Sayed, M. Y., DeBose, C. D., Coury, L. A., & Roberts, M. F. (1985) *Biochim. Biophys. Acta 837*, 325–335.
Finer, E. G., Flook, A. G., & Hauser, H. (1972) *Biochim. Biophys. Acta 260*, 49–58.
Fobes, J., Husted, C., & Oldfield, E. (1988) *J. Am. Chem. Soc. 110*, 1059–1065.
Gabriel, N. E., & Roberts, M. F. (1987) *Biochemistry 26*, 2432–2440.
Halladay, H. N., Stark, R. E., Ali, S., & Bittman, R. (1990) *Biophys. J. 58*, 1449–1461.
Helfrich, W. (1974) *Phys. Lett. 50A*, 115–116.
Helm, C. A., Israelachvili, J. N., & McGuiggan, P. M. (1992) *Biochemistry 31*, 1794–1805.

Hermann, D., Bosies,E., Zilch, H., & Koch, E. (1992) U.S. Patent 572,475.
Heuckeroth, R. O., & Gordon, J. I. (1989) *Proc. Natl. Acad. Sci. U.S.A. 86*, 5262–5266.
Heuckeroth, R. O., Glaser, L., & Gordon, J. I. (1988) *Proc. Natl. Acad. Sci. U.S.A. 85*, 8795–8799.
Huang, C., & Mason, J. T. (1978) *Proc. Natl. Acad. Sci. U.S.A. 75*, 308–310.
Israelachvilli, J. N., & Mitchell, D. L. (1975) *Biochem. Biophys. Acta 389*, 13–19.
Jonas, J., Winter, R., Grandinetti, P. J., & Driscoll, D. (1990) *J. Magn. Reson. 87*, 536–547.
Kumar, R., Gardner, M. F., Richman, D. D., & Hostetler, K. Y. (1992) *J. Biol. Chem. 267*, 20288–20292.
Lasic, D. D. (1988) *Biochem. J. 256*, 1–11
Lipowsky, R. (1991) *Nature 349*, 475–481.
Macur, S., Farmer, B. T., II, & Brown, L. R. (1986) *J. Magn. Reson. 70*, 493–499.
Menger, F. M., Wood, M. G., Jr., Zhou, Q. Z., Hopkins, H. P., & Fumero, J. (1988) *J. Am. Chem. Soc. 110*, 6804–6810.
Nayar, R., Hope, M. J., & Cullis, P. R. (1989) *Biochim. Biophys. Acta 986*, 200–206.
Ohki, S. (1982) *Biochim. Biophys. Acta 689*, 1–11.
Pidgeon, C., & Hunt, C. A. (1981) *J. Pharm. Sci. 70*, 173–176.
Pidgeon, C., & Venkatarum, U. V. (1989) *Anal. Biochem. 176*, 36–47.
Pidgeon, C., Hunt, A. H., & Dittrich, K. (1986) *Pharm. Res. 3*, 23–34.
Pidgeon, C., McKneely, S., Schmidt, S., & Johnson, J. E. (1987) *Biochemistry 26*, 17–29.
Pidgeon, C., Markovich, R. J., Liu, M. D., Holzer, T., Novak, R., & Keyer, K. (1993) *J. Biol. Chem. 268*, 7773–7778.
Qiu, X., Mirau, P. M., & Pidgeon, C. (1993) *Biochem. Biophys. Acta 1147*, 59–72.
Rance, M., & Byrd, R. A. (1983) *J. Magn. Reson. 52*, 221–240.
Reinl, H., Brumm, T., & Bayer, T. M. (1992) *Biophys. J. 61*, 1025–1035.
Schuh, J. R., Luciano, B., Muller, L., & Chan, S. I. (1982) *Biochim. Biophys. Acta 687*, 219–225.
Schullery, S. E., Schmidt, C. F., Felgner, P., Tillack, T. W., & Thompson, T. E. (1980) *Biochemistry 19*, 3919–3923.
Seddon, J. (1990) *Biochim. Biophys. Acta 1031*, 1–69.
Seelig, J. (1978) *Biochim. Biophys. Acta 515*, 105–140.
Siegel, D. P. (1987) in *Cell Fusion* (Sowers, A. E., Ed.) Plenum, New York.
Siegel, D. P., Burns, J. L., Chestnut, M. H., & Talmon, Y. (1989) *Biophys. J. 56*, 161–169.
Stark, R. E., Storrs, R. W., Levine, S. E., Yee, S., & Broido, M. S. (1986) *Biochim. Biophys. Acta 860*, 399–410.
States, D. J., Haberkorn, R. A., & Ruben, D. J. (1982) *J. Magn. Reson. 48*, 286–292.
Vold, R. L., Waugh, J. S., Klein, M. P., & Phelps, D. E. (1968) *J. Chem. Phys. 48*, 3831–3832.
Walter, A., Vinson, P. K., Kaplun, A., & Talmon, Y. (1991) *Biophys. J. 60*, 1315–1325.
Xu, Z.-C., & Cafiso, D. S. (1986) *Biophys. J. 49*, 779–783.
Yeagle, P., Young, J., Hui, S. W., & Epand, R. M. (1992) *Biochemistry 31*, 3177–3183.